

ANALYSIS OF BREAKDOWN DAMAGE IN AN 805 MHz PILLBOX CAVITY FOR MUON IONIZATION COOLING R&D*

D. Bowring[†], D. Li, LBNL, Berkeley, CA, USA
A. Moretti, Y. Torun, FNAL, Batavia, IL, USA

Abstract

When operating in multi-Tesla solenoidal magnetic fields, normal-conducting cavities exhibit RF breakdown at anomalously low gradients. This breakdown behavior may be due to field-emitted electrons, focused by the magnetic field into beamlets with relatively large current densities. These beamlets may then cause pulsed heating and cyclic fatigue damage on cavity interior surfaces [1]. It follows that materials with long radiation lengths (relative to copper) may alleviate the problem of RF breakdown in strong magnetic fields. To study this phenomenon, RF breakdown was induced on pairs of “buttons” in an 805 MHz pillbox cavity. The shape of the buttons creates a local enhancement of the surface electric field, such that breakdown occurs preferentially on the button surface. Beryllium and copper buttons were tested in order to evaluate the effect of material choice on RF breakdown performance. This poster presents an analysis of the damage to these buttons and suggests a path forward for future materials R&D related to breakdown in strong magnetic fields.

INTRODUCTION

Ionization cooling is the preferred method for quickly achieving the required transverse emittance during the acceleration of muon beams [2, 3, 4]. In an ionization cooling channel, low-Z absorber sections isotropically attenuate beam momentum, and normal-conducting RF cavities replace only the longitudinal momentum. The RF cavities are placed in multi-Tesla magnetic fields for beam confinement and radial focusing.

Various copper RF cavities have exhibited an increased incidence of RF breakdown rates in the presence of a multi-Tesla solenoidal magnetic field [5]. In these cavities, the maximum achievable surface electric field decreases as the applied solenoidal field increases from 0 to 4 Tesla [6]. The sparks from RF breakdown events damage the cavity, which likely leads to further reductions in the maximum achievable gradient for a given magnetic field.

Several cavities have been tested in order to study this phenomenon [7]. We discuss here the results from tests of an 805 MHz pillbox cavity. Breakdown was observed in various magnetic field strengths and for various cathode

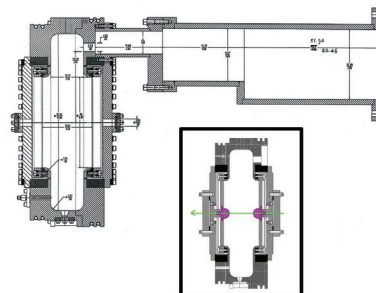


Figure 1: Schematic of the 805 MHz pillbox cavity. The gap length is 81 mm and the radius is 158 mm. The inset shows the cavity with buttons installed (purple) and the direction of the applied magnetic field (green).

materials. The resulting cavity damage has been characterized, and we have made estimates of breakdown current density and duration based on this damage.

THE 805 MHz PILLBOX CAVITY

RF measurements were made using a pillbox-type 805 MHz cavity with Cu walls [5]. A cavity schematic is shown in Figure 1. Note that the cavity is magnetically coupled through a slot in one of the end walls. The longitudinal magnetic field is applied by placing the cavity in the 44-cm-diameter warm bore of a superconducting solenoid. The cavity is side-coupled, then, in order to fit the waveguide and associated RF apparatus inside the magnet. Two buttons are installed on opposite sides of the cavity, as shown in the inset in Figure 1. These buttons are hemispherical, with a 12.7 mm radius. The geometric field enhancement on the button surface serves to localize RF breakdown events. This field enhancement is illustrated in Figure 2. Since the buttons are replaceable, different materials and surface treatments may be evaluated.

RF MEASUREMENTS

10^{-5} sparks per RF pulse is deemed to be an acceptable trip rate in an eventual muon ionization cooling channel, and so this spark rate is used to establish an upper limit for operating gradients. RF power was delivered in 20 μ s pulses at a repetition rate of 10 Hz. Maximum achievable cavity gradients are listed in Table 1 for various magnetic field strengths. Beryllium and copper buttons were tested in this way. Relative to Cu, Be has a longer radiation length

* This work was supported by the Office of Science, U.S. Department of Energy under DOE contract number DE-AC02-05CH11231.

[†] dbowring@lbl.gov

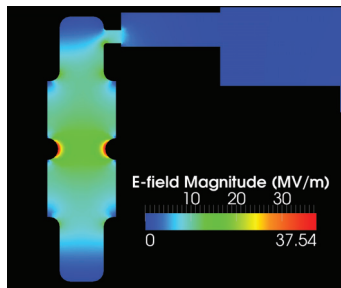


Figure 2: Simulation of the electric field inside the 805 MHz pillbox cavity, using SLAC's ACE3P code suite [8].

Table 1: Maximum Achievable Cavity Gradient

Magnetic Field (T)	Max. gradient for Cu (MV/m)	Max. gradient for Be (MV/m)
0	35	40
1.5	33	30
3	31	28

and a higher melting temperature and so may be more resistant to damage from breakdown events [1]. The Be buttons were coated with thin TiN films in order to suppress multipacting. For the purposes of this analysis, the button on the cavity wall closest to the coupling iris is denoted the “upstream” button and the opposing button is denoted “downstream”.

Due to time and operational constraints, buttons were not inspected after every experimental run at each magnetic field strength. It is therefore impossible at present to associate specific damage sites with specific gradient and magnetic field values. We have designed and are currently fabricating a modular pillbox cavity that will enable rapid, easy inspection of cavity surfaces [9]. Further button tests will be conducted using this cavity, allowing frequent inspections during testing and, consequently, the time-dependent mapping of breakdown damage.

BREAKDOWN DAMAGE

Damage Characterization

Photographs in Figure 3 show the surfaces of Cu and Be buttons after measurement. Note that although both buttons were damaged by spark events, damage on the Be button is microscopic. See Figure 5.

Microscopic imaging was conducted using a Keyence VK-9700 laser confocal scanning microscope (LCSM). The LCSM and its associated analysis software enables measurements of surface roughness and the depth (or height), diameter, and volume of individual damage sites.

Damage on Cu Buttons

Breakdown arcs leave craters on the Cu button surfaces. A typical crater is shown in Figure 4. Approximately 200



Figure 3: Photos of a Cu (left) and Be (right) button after high-power RF testing. μm -scale damage is present on the Be button surface, but is not visible to the naked eye. Damage on the Cu button is mm-scale.

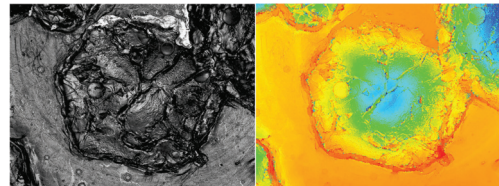


Figure 4: Typical LCSM images of damage on a Cu button. The right-hand image is a false-color map containing height information. Warm colors (red, orange) are closer to the camera than cool colors (blue, green). This crater has a maximum depth of $73.79 \pm 0.01 \mu\text{m}$, an effective diameter at the rim of $430 \mu\text{m}$, and a volume of $(2.592 \pm 0.002) \times 10^6 \mu\text{m}^3$.

such craters were characterized on the upstream and downstream Cu buttons using the LCSM. Virtually all craters exhibit the same general characteristics: a raised lip around the crater rim; a rough, cracked interior; and solidified droplets of Cu indicative of energetic arc processes in the vicinity of liquid metal.

The average crater diameter is $(4 \pm 1) \times 10^2 \mu\text{m}$, with no significant difference in crater size between upstream and downstream buttons. We find no correlation between crater size and its position on a button. This is likely because surface roughness and contamination play a significant role in cathode arc processes [12]. Such properties are position-independent in this case. Furthermore, there is presently no way to associate crater size with gradient or solenoidal field values at the time that crater is formed.

Damage on Be Buttons

The Be buttons are more difficult to characterize. The average damage site has a diameter of $10 \pm 6 \mu\text{m}$, with an average volume of $50 \pm 70 \mu\text{m}^3$. The integrated mean surface roughness of the undamaged Be was measured to be $R_a = 4.60 \mu\text{m}$ and the ten-point mean roughness $R_z = 123.10 \mu\text{m}$. This makes it difficult to distinguish breakdown damage from normal button roughness, and accounts for the spread in volume data cited above. Identification of breakdown damage is simplified in some cases because arcs may ablate the TiN button coatings, highlighting arc impact sites as in Figure 5. However, this ablation does not happen consistently and cannot be used in all cases to identify breakdown craters. In the future, Be buttons should be polished to μm -scale surface roughness to avoid such problems.

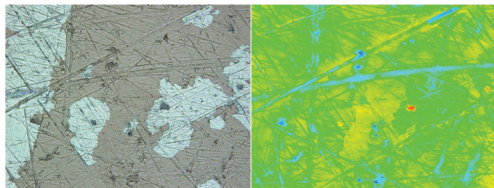


Figure 5: LCSM images of damage on a Be button. Damage sites may be concave (as for Cu damage) or convex. X-ray diffractometry reveals the light patches as bare Be, after the TiN film was vaporized during breakdown events. Note that TiN is not missing in the vicinity of every damage site.

ANALYSIS AND CONCLUSIONS

A typical approach to breakdown in RF cavities is to start with field emission models that require specific current densities and then to examine the cavity surface for geometric features that would give rise to those current densities [10, 11]. This approach is complicated by the likelihood that the surface features enabling explosive electron emission are destroyed during the emission process. A complementary method involves estimation of current densities based on the size of arc damage spots.

Models of crater formation based on Joule heating give relationships between arc current I , crater formation time τ , and crater radius r [12, 13, 14]:

$$r = r_0 e^{I/I_0} \quad (1)$$

$$r^2/\tau = 13 \text{ cm}^2/\text{s} \quad (2)$$

where r_0 , I_0 , and the proportionality constant in Equation 2 are empirically determined. Arc current¹ densities are then estimated by assuming arc spot size is equivalent to the resultant crater size. Note that a Gaussian distribution of crater radii result from a single arc current value, likely due to contributions from surface contamination. A more precise determination of I from measured r values in this case will require more data. Using these models, we estimate for the Cu buttons that current densities range from 10^9 to 10^{11} A/m², and that craters form in tens of μs .

Compare this μs -scale crater formation time with the time required for the cavity's stored energy to fall to zero after a spark – typically on the order of ns. It may be that a Joule heating model alone is not sufficient to explain crater formation in S-band RF cavities. The next step in this analysis will be an evaluation of more complete arc models, in which crater evacuation is accelerated by plasma pressure at the cathode spot and its various hydrodynamic consequences [15].

There is considerably less information in the literature about arc damage on beryllium cathodes. General models

¹Guile and Jüttner argue that cathode arcs and breakdown events are similar enough that they may be treated by the same model [12].

of arc processes exist, and we may develop these models for future studies of breakdown on Be surfaces [16].

The button measurements suggest that Be is indeed less susceptible to breakdown damage than Cu, if damage is quantified by the volume of removed material during a spark. More statistics will be necessary in order to determine conclusively whether this μm -scale damage lowers a cavity's maximum achievable gradient, independent of the magnetic field effects discussed above.

Finally, this approach to the characterization of breakdown damage will inform the approach to fabrication and testing of the new modular pillbox cavity [9]. That cavity will allow in-situ optical measurements which may experimentally confirm arc duration times. Furthermore, frequent inspections of the cavity will allow individual damage sites to be associated with specific gradients and magnetic field strengths. Data from the modular cavity, along with the microscopy and crater erosion analyses discussed here, should yield a very complete picture of breakdown in strong magnetic fields.

ACKNOWLEDGMENT

We would like to thank D. Hicks and A. Romanenko for their assistance with the microscopy facilities at FNAL.

REFERENCES

- [1] D. Stratakis, J.C. Gallardo, and R.B. Palmer, Nucl. Inst. Meth. A 620 (2010), 147-154.
- [2] R. Palmer et al., AIP Conf. Proc. 441 (1998) 183.
- [3] C. Ankenbrandt et al., PRST-AB 2 (1999) 8.
- [4] A. Blondel et al., "MICE, The International Muon Ionization Cooling Experiment," TUPFI046, these proceedings.
- [5] R.B. Palmer et al., PRST-AB 12 (2009) 031002.
- [6] D. Huang et al., "RF studies at Fermilab MuCool Test Area," PAC09, Vancouver, May 2009, TU5PFP032, p. 888, <http://www.JACoW.org>
- [7] K. Yonehara et al., "Recent progress of RF cavity study at MuCool Test Area," NuFact11, Geneva, Switzerland, 2011, FERMILAB-CONF-11-639-APC.
- [8] K. Ko et al., "Advances in parallel electromagnetic codes for accelerator science and development," LINAC2010, Tsukuba, Japan.
- [9] D. Bowring et al., "A modular cavity for muon ionization cooling R&D," WEPFI073, these proceedings.
- [10] J. Wang and G. Loew, "RF breakdown studies in copper electron linac structures," 1989, Chicago, IL, USA, pp. 1137-1139, <http://www.JACoW.org>
- [11] A. Descoedres, PRST-AB 12 (2009) 092001.
- [12] A.E. Guile and B. Jüttner, IEEE Trans. Plasma Sci. PS-8 (1980) 3.
- [13] J.E. Daalder, IEEE Trans. Power. App. Syst. 93 (1974) p. 747.
- [14] B. Jüttner, Beitr. Plasmaphys. 19 (1979) 1, pp. 25-48.
- [15] E. Hantzsche, Beitr. Plasmaphys. 17 (1977) p. 65.
- [16] E. Hantzsche and B. Jüttner, IEEE. Trans. Plasma Sci. 13 (1985) 5.